

# C++ implementation of the solution of incompressible viscous time-dependent Navier-Stokes equations using projection method in Dealii

Muhammad Mohebujjaman <sup>\*</sup>      Timo Heister <sup>†</sup>

MTHSC9830 Spring 2015 Project

## Abstract

In this project, we implement the projection method algorithm in dealii [1] with multithreading. This work is an extension of dealii example step-35. Calculating right hand side function for a true solution from Navier-Stokes equation, we implement the right side function and known boundary value function into our code. We checked the convergence rate with respect to different norms for velocity and pressure for the algorithm. Finally we plot some graphs for velocity and pressure at different times with some specified values of the parameter.

## 1 Introduction

We know that in numerical simulation of time-dependent viscous incompressible flows the velocity and pressure are coupled by the incompressibility constraint. This is one of the major difficulty in solving time-dependent Navier-Stokes equations [3]. To overcome this difficulty in time-dependent problem, the interest of using projection methods started in the late 1960s. This method was originally introduced by Alexandre Chorin [2] as an efficient means of solving time-dependent Navier-Stokes equations. The key advantage feature of projection methods is that, at each time step, one only needs to solve a sequence of decoupled elliptic equations for the velocity and the pressure, making it very efficient for large scale numerical simulations. The equations describe the flow of an unsteady viscous incompressible fluid are given by

$$u_t + u \cdot \nabla u - \nu \Delta u + \nabla p = f \text{ in } \Omega \times [0, T] \quad (1)$$

$$\nabla \cdot u = 0 \text{ in } \Omega \times [0, T] \quad (2)$$

$$u|_{t=0} = u_0 \text{ in } \Omega, \quad (3)$$

$$u|_{\partial\Omega} = u_b \text{ in } [0, T] \quad (4)$$

---

<sup>\*</sup>Department of Mathematical Sciences, Clemson University, Clemson, SC, 29634; mmo-hebu@g.clemson.edu

<sup>†</sup>Department of Mathematical Sciences, Clemson University, Clemson, SC, 29634. heister@clemson.edu

Where  $u$  represents the velocity of the flow,  $p$  is the pressure,  $f$  is a smooth forcing term,  $\nu$  is the kinematic viscosity,  $\Omega$  is the domain,  $u_0$  is an initial velocity field. For the time-dependent case, after the time discretization, we would arrive a system like

$$\begin{aligned}\frac{1}{\Delta t}u^k - \nu\Delta u^k + \nabla p^k &= F^k \\ \nabla \cdot u &= 0\end{aligned}$$

where  $\Delta t$  is the time-step. This could be solved using a Schur complement approach as the structure of this system is pretty similar to the Stokes system. But the condition number of the Schur complement is proportional to  $(\Delta t)^{-2}$ . Therefore, for small  $\Delta t$ , the condition number becomes very high and this makes the system very difficult to solve and so for the time-dependent Navier-Stokes equations, Schur complement approach is not a useful avenue to the solution.

## 2 Notations and Preliminaries

We consider the time-dependent Navier-Stokes equations on a finite time interval  $[0, T]$  and in an open, connected, bounded Lipschitz domain  $\Omega \subset \mathbb{R}^d, d \in 2, 3$ . We denote the usual  $L^2(\Omega)$  norm and its inner product by  $\|\cdot\|$  and  $(\cdot, \cdot)$  respectively. The  $L^p(\Omega)$  norms and the Sobolev  $W_p^k(\Omega)$  norms are denoted by  $\|\cdot\|_{L^p}$  and  $\|\cdot\|_{W_p^k(\Omega)}$  respectively for  $k \in \mathbb{N}, 1 \leq p \leq \infty$ . In particular,  $H^k(\Omega)$  is used to represent the Sobolev space  $W_2^k(\Omega)$ .  $\|\cdot\|_k$  and  $|\cdot|_k$  denote the norm and the seminorm in  $H^k(\Omega)$ . For  $X$  being a normed function space in  $\Omega$ ,  $L^p(0, T; X)$  is the space of all functions defined on  $[0, T] \times \Omega$  for which the norm

$$\|u\|_{L^p(0, T; X)} = \left( \int_0^T \|u\|_X^p dx \right)^{1/p}, p \in [1, \infty)$$

is finite. For  $p = \infty$ , the usual modification is used in the definition of this space.

## 3 Projection Methods

As we have already discussed that the difficulty in the solution of the time-dependent Navier-Stokes equations comes from the fact that the velocity and the pressure are coupled through the incompressibility constraint

$$\nabla \cdot u = 0,$$

for which the pressure is the Lagrange multiplier. Projection methods aim at decoupling the constraint from the diffusion operator. The algorithm for the projection methods is as follows:

Step 1: Compute an intermediate velocity  $u^*$  by ignoring pressure term and incompressibility. Solve the time discretized equation.

Step 2: Perform a step which involves a Poisson equation for pressure, and is equivalent to a projection of  $u^*$  onto the div free space.

Note that we change the advection term  $u \cdot \nabla u$  by its skew symmetric form  $u \cdot \nabla u + \frac{1}{2}(\nabla \cdot u)u$  which is consistent with the continuous case as  $\nabla \cdot u = 0$  but this may not be true for pointwise for the discrete solution. But this skew symmetric form is essential to have an unconditional stability of the time-stepping scheme. To avoid non-linearity in the advection term, we use the second order extrapolation  $u^*$  of  $u^{k+1}$ .

To obtain a fully discrete setting of the projection method, we multiply both sides of (1) from right by the test vector  $v$  and integrate by parts. That is, we have some steps as follows:

$$-\nu \int_{\Omega} \Delta u \cdot v \, d\Omega$$

For the Dirichlet boundary conditions on the whole boundary, we have

$$-\nu \int_{\Omega} \Delta u \cdot v \, d\Omega = -\nu \int_{\partial\Omega} \nabla u \cdot n \, v \, dS + \nu \int_{\Omega} \nabla u \cdot \nabla v \, d\Omega = \nu \int_{\Omega} \nabla u \cdot \nabla v \, d\Omega$$

In this formulation the velocity components are fully decouples. But for non-standard boundary conditions, we can use the following identity

$$\Delta u = \nabla \nabla \cdot u - \nabla \times \nabla \times u$$

Integrating by parts and taking into account the boundary conditions we have

$$-\nu \int_{\Omega} \Delta u \cdot v \, d\Omega = \nu \int_{\Omega} (\nabla \cdot u \nabla \cdot v + \nabla \times u \nabla \times v) \, d\Omega$$

This couples the components of the velocity vector. For pressure boundary condition, we need to write the following

$$\int_{\Omega} \nabla p \cdot v \, d\Omega = \int_{\partial\Omega} p \, v \cdot n \, dS - \int_{\Omega} p \nabla \cdot v \, d\Omega = - \int_{\Omega} p \nabla \cdot v \, d\Omega$$

Where the boundary integral equals zero due to the pressure boundary condition.

Now we will describe how the projection methods look like in a semi-discrete setting. Our aim is to obtain a sequence of velocities  $u^k$  and pressures  $p^k$ . We will also obtain a sequence  $\phi^k$  of auxiliary variables. Suppose that from the initial conditions we have  $u^0, p^0$  and setting  $\phi^0 = 0$ . Using a first order method we can find  $u^1, p^1$  and setting  $\phi^1 = p^1 - p^0$ . Then the projection method for the governing equations (1)-(4) consists of the following steps:

**Step 0:** Extrapolation. Define

$$u^* = 2u^k - u^{k-1}, \quad p^\# = p^k + \frac{4}{3}\phi^k - \frac{1}{3}\phi^{k-1}$$

**Step 1:** Diffusion step. Find  $u^{k+1}$  solving the single linear equation

$$\frac{1}{2\Delta t}(3u^{k+1} - 4u^k + u^{k-1}) + u^* \cdot \nabla u^{k+1} + \frac{1}{2}(\nabla \cdot u^*)u^{k+1} - \nu \Delta u^{k+1} + \nabla p^\# = f^{k+1}$$

$$u^{k+1}|_{\partial\Omega} = u_b$$

**Stpe 2:** Projection. Find  $\phi^{k+1}$  that solves

$$\Delta\phi^{k+1} = \frac{3}{2\tau}\nabla \cdot u^{k+1}, \quad \partial_n\phi^{k+1}|_{\partial\Omega} = 0$$

**Stpe 3:** Pressure correction. Here we have two options:

- Incremental Method in Standard Form

$$p^{k+1} = p^k + \phi^{k+1}$$

- Incremental Method in Rotational Form

$$p^{k+1} = p^k + \phi^{k+1} - \nu\nabla \cdot u^{k+1}$$

## 4 Numerical Experiments

In this section, we run numerical experiment in dealii [1] with multi-threading to test the proposed scheme. We will verify predicted convergence rates for velocity and pressure with respect to different norms. For all our simulations, we choose  $(Q_2, Q_1)$  elements.

### 4.1 Convergence rate verification

To exhibit the effectiveness of the projection method with BDF2 time stepping scheme, we compute convergence rates on a series of refined meshes and timesteps. We choose the test problem with solution

$$v = \begin{pmatrix} \cos y + (1 + e^t) \sin y \\ \sin x + (1 + e^t) \cos x \end{pmatrix}, \quad p = \sin(x + y)(1 + e^t)$$

on a rectangular domain  $\{(x, y) : 0 \leq x \leq 1, 0 \leq y \leq 1\}$  and the right hand side function  $f$  is calculated accordingly.

$$p' = p - p_{mean} \text{ and } p'_h = p_h - p_{hmean}$$

## 5 Conclusion

The project was basically writing code for the projection method. We did not prove the convergence rate for the algorithm theoretically. The velocity convergence rates as varying time steps what we get from running our code are 2, 1.82 and 2 with respect to  $\|\cdot\|_{L^2(0,T;L^2)}$ ,  $\|\cdot\|_{L^2(0,T;H^1)}$  and  $\|\cdot\|_{L^2(0,T;L^\infty)}$  norms respectively. Varying mesh widths, the found velocity convergence rates are 3, 2 and 3 with respect to  $\|\cdot\|_{L^2(0,T;L^2)}$ ,  $\|\cdot\|_{L^2(0,T;H^1)}$  and  $\|\cdot\|_{L^2(0,T;L^\infty)}$  norms respectively. The pressure convergence rates 1.9 and 2 for varying time steps and mesh widths respectively. The obtained convergence rates for velocity and pressure seem reasonable with respect to the available theory in literature for the projection methods.

$\Delta t$	$\ u - u_h\ _{2,2}$	Rate	$\ u - u_h\ _{2,1}$	Rate	$\ u - u_h\ _{\infty,2}$	Rate
$\frac{T}{2}$	0.122286		0.821992		0.172938	
$\frac{T}{4}$	0.0424948	1.5249	0.241278	1.7684	0.0679916	1.3468
$\frac{T}{8}$	0.0140192	1.5999	0.0784814	1.6203	0.0198712	1.7747
$\frac{T}{16}$	0.00391612	1.8399	0.0261534	1.5854	0.00597801	1.7329
$\frac{T}{32}$	0.00103406	1.9211	0.00778855	1.7476	0.00157841	1.9212
$\frac{T}{64}$	0.000266434	1.9565	0.00222171	1.8097	0.000409103	1.9479
$\frac{T}{128}$	6.77244e-05	1.9760	0.000625176	1.8293	0.000104284	1.9719
$\frac{T}{256}$	1.70838e-05	1.9870	0.000176967	1.8208	2.63378e-05	1.9853

Table 1: Velocity convergence rates for  $\nu = 0.1$ , fixed end time  $T = 1.0$ , fixed number of refinement 6 with  $(Q_2, Q_1)$  elements and varying timesteps.

# Ref.	$\ u - u_h\ _{2,2}$	Rate	$\ u - u_h\ _{2,1}$	Rate	$\ u - u_h\ _{\infty,2}$	Rate
1	3.04545e-05		0.000395489		0.00103236	
2	3.99087e-06	2.9319	0.000101963	1.9556	0.000138586	2.8971
3	4.95461e-07	3.0099	2.59035e-05	1.9768	1.70667e-05	3.0215
4	6.23184e-08	2.9910	6.47765e-06	1.9996	2.14725e-06	2.9906
5	7.76263e-09	3.0050	1.61257e-06	2.0061	2.63869e-07	3.0246
6	1.00147e-09	2.9544	3.98647e-07	2.0162	3.53456e-08	2.9002

Table 2: Velocity convergence rate for  $\nu = 0.1$ , fixed end time  $T = 0.001$ , fixed time step  $\Delta t = T/8$ , with  $(Q_2, Q_1)$  elements and varying mesh widths.

$\Delta t$	$\ p' - p'_h\ _{2,2}$	Rate	# of Ref.	$\ p' - p'_h\ _{2,2}$	Rate
$\frac{T}{2}$	0.113634		1	0.00200424	
$\frac{T}{4}$	0.0877048	0.3737	2	0.000521994	1.9410
$\frac{T}{8}$	0.0456035	0.9435	3	0.000125518	2.0561
$\frac{T}{16}$	0.0135359	1.7524	4	3.13784e-05	2.0001
$\frac{T}{32}$	0.00365159	1.8902	5	7.84443e-06	2.0000
$\frac{T}{64}$	0.000952086	1.9394	6	1.9611e-06	2.0000
$\frac{T}{128}$	0.000258669	1.8800	7	4.96725e-07	1.9811

Table 3: Pressure convergence rates for  $\nu = 0.1$ ,  $(Q_2, Q_1)$  elements (1) fixed end time  $T = 1.0$ , fixed number of refinement 6 with varying timesteps and (2) with fixed end time  $T = 0.001$ ,  $\Delta t = T/8$  with varying mesh widths.

## References

- [1] W. Bangerth, D. Davydov, T. Heister, L. Heltai, G. Kanschat, M. Kronbichler, M. Maier, B. Turcksin, and D. Wells. The `deal.II` library, version 8.4. *Journal of Numerical Mathematics*, 24, 2016.

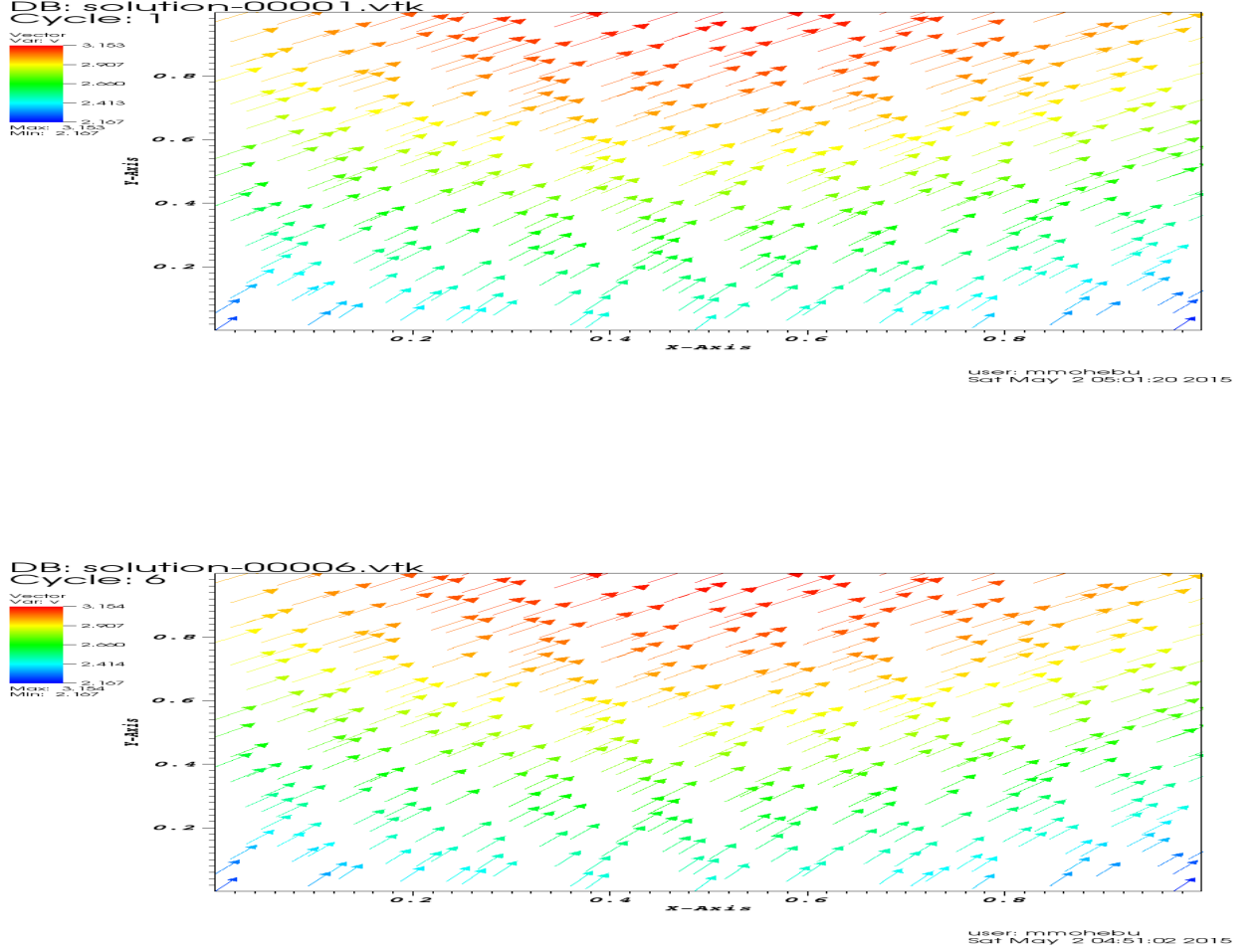


Figure 1: Velocity vector plot at  $t = 0.0$  (top) and at  $t = 0.00075$  where  $\nu = 0.1$ , final time  $T = 0.001$ ,  $\Delta t = 0.000125$ , number of mesh refinement 6.

- [2] A.J. Chorin. Numerical solution of the navier-stokes equations. *Mathematics of Computation*, 22:745–762, 1968.
- [3] J.L. Guermond, P. Mineev, and J. Shen. An overview of projection methods for incompressible flows. *Computer Methods in Applied Mechanics and Engineering*, 195:6011–6045, 2006.

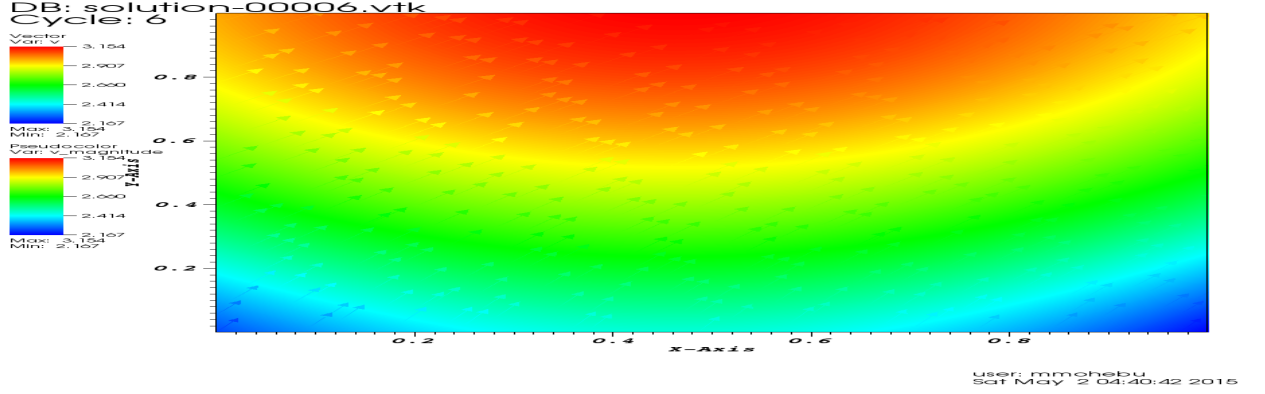


Figure 2: Velocity vector plot with its magnitude (bottom) at  $t = 0.00075$  where  $\nu = 0.1$ , final time  $T = 0.001$ ,  $\Delta t = 0.000125$ , number of mesh refinement 6.

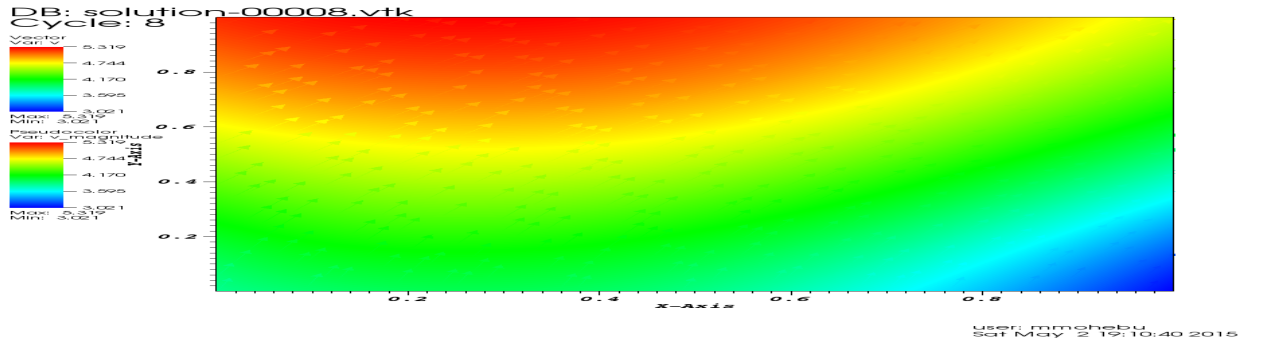


Figure 3: Velocity vector plot with its magnetitude at  $t = 1.0$  where  $\nu = 0.1$ , final time  $T = 1$ ,  $\Delta t = 0.125$ , number of mesh refinement 6.

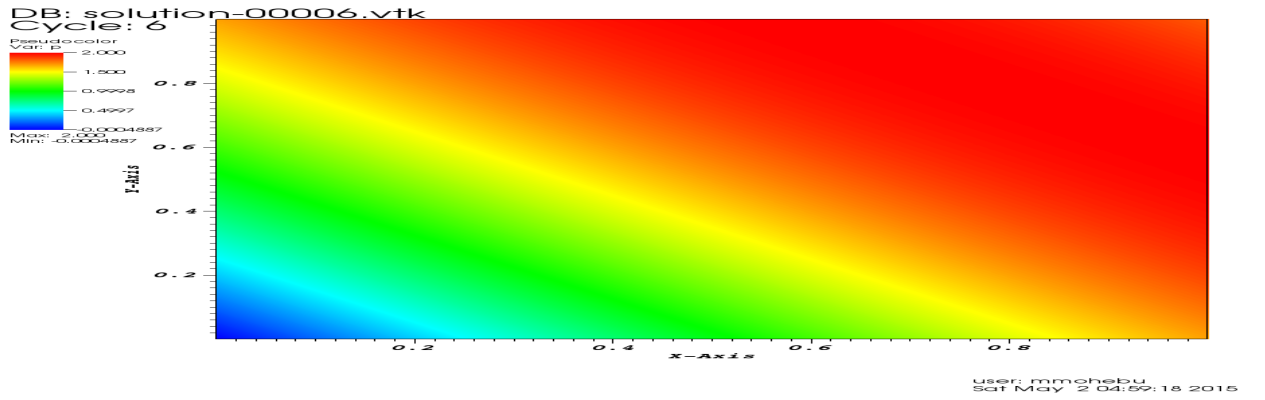
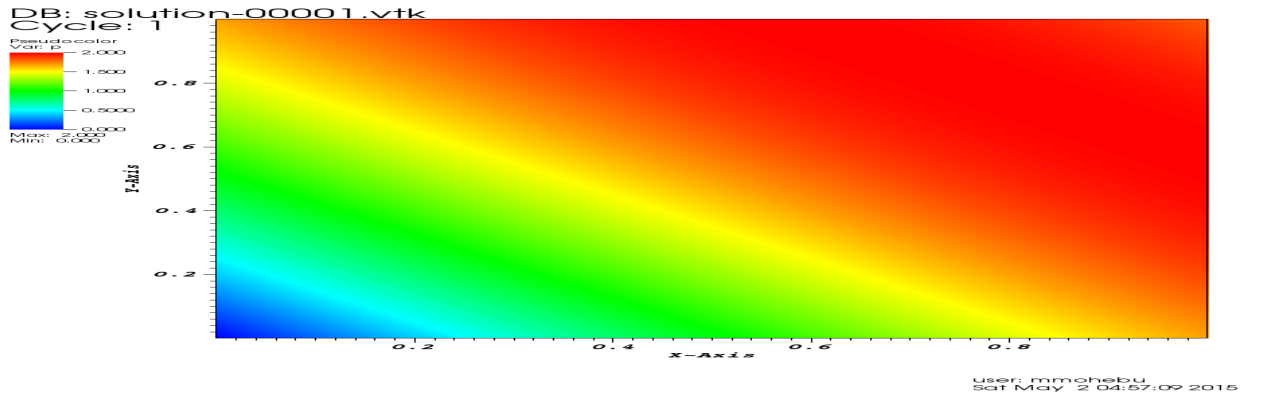


Figure 4: pressure function plot at  $t = 0.0$  (top) and at  $t = 0.00075$  (bottom) where  $\nu = 0.1$ , final time  $T = 0.001$ ,  $\Delta t = 0.000125$ , number of mesh refinement 6.



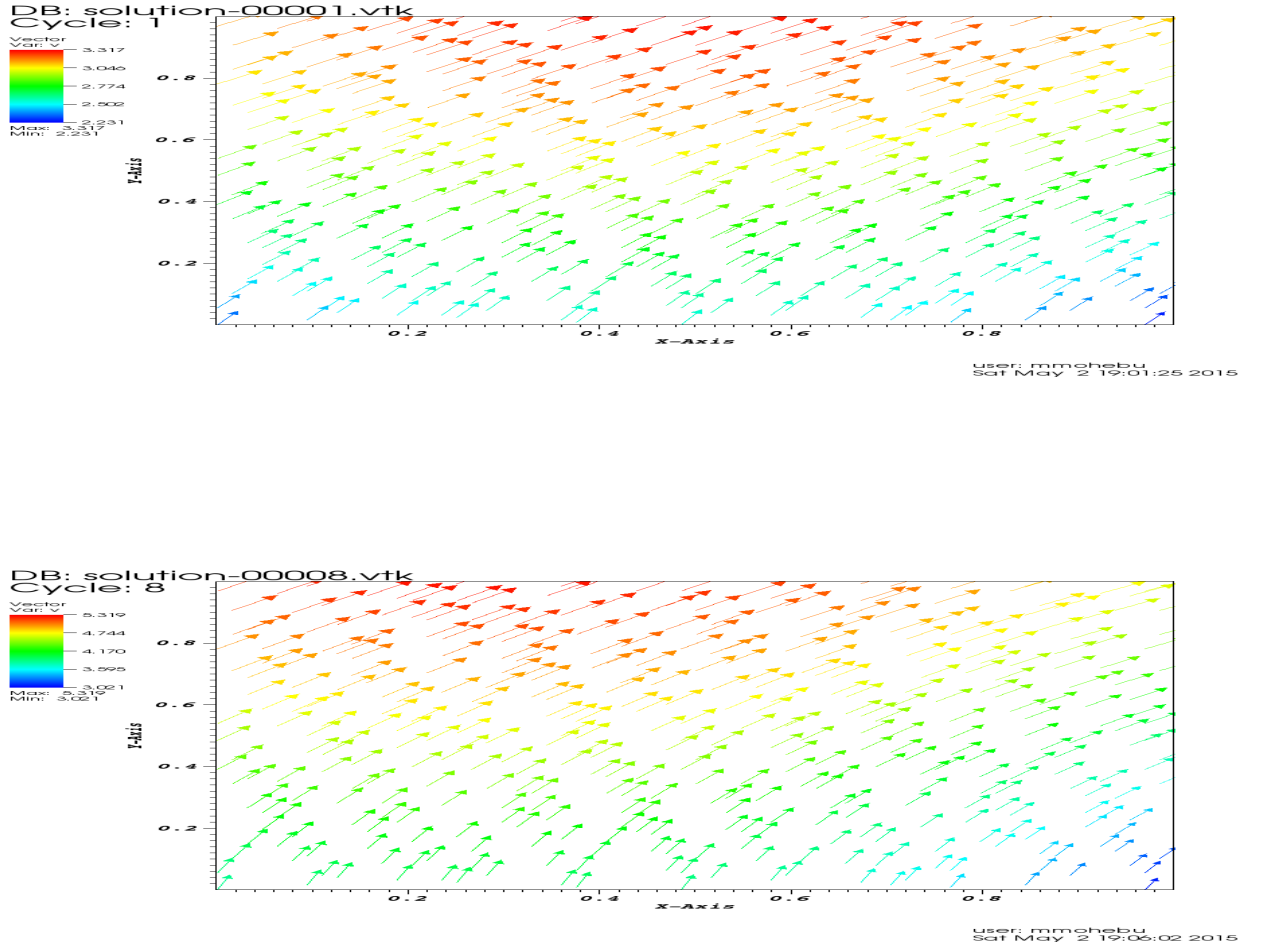


Figure 5: Velocity vector plot at  $t = 0.0$  (top) and at  $t = 1.0$  (bottom) where  $\nu = 0.1$ , final time  $T = 1.0$ ,  $\Delta t = 0.125$ , number of mesh refinement 6.

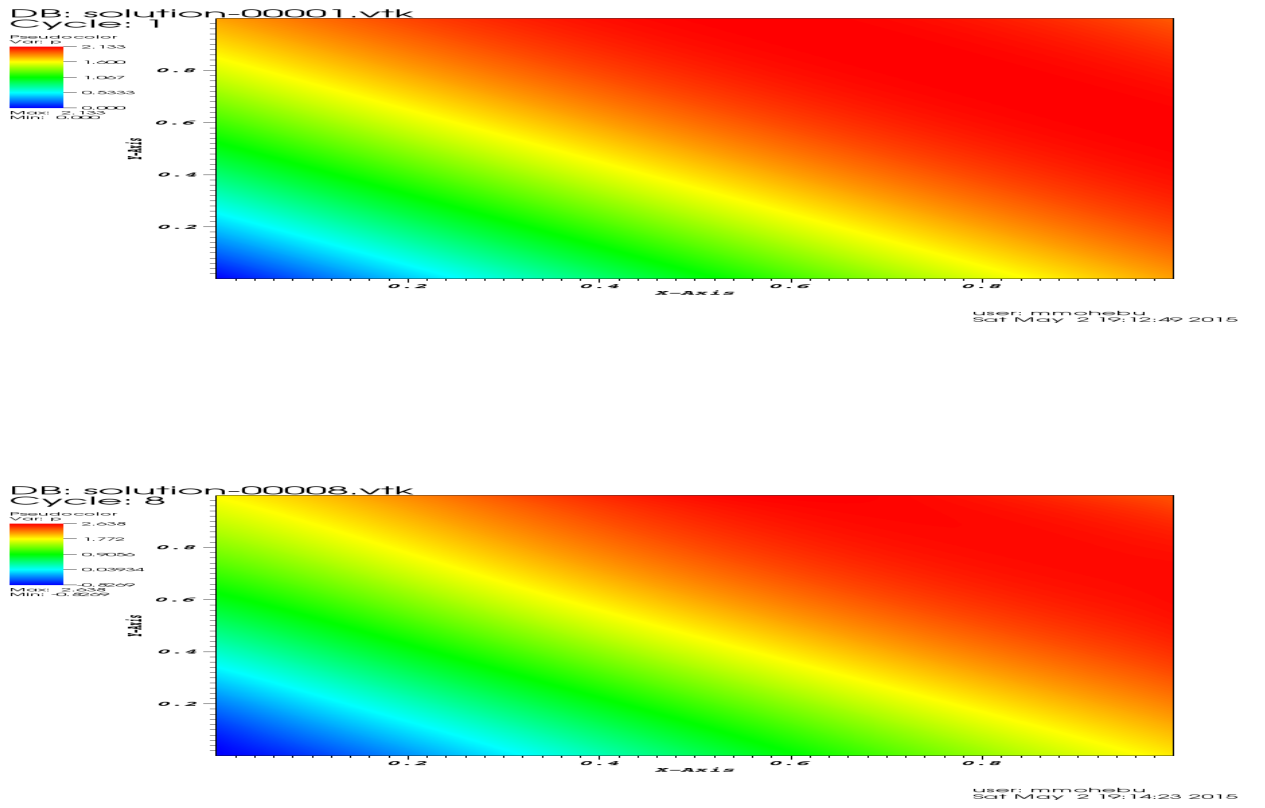


Figure 6: pressure function plot at  $t = 0.0$  (top) and at  $t = 1.0$  (bottom) where  $\nu = 0.1$ , final time  $T = 1$ ,  $\Delta t = 0.125$ , number of mesh refinement 6.